Communications in Applied Mathematics and Computational Science

Volume 2 No. 1 2007

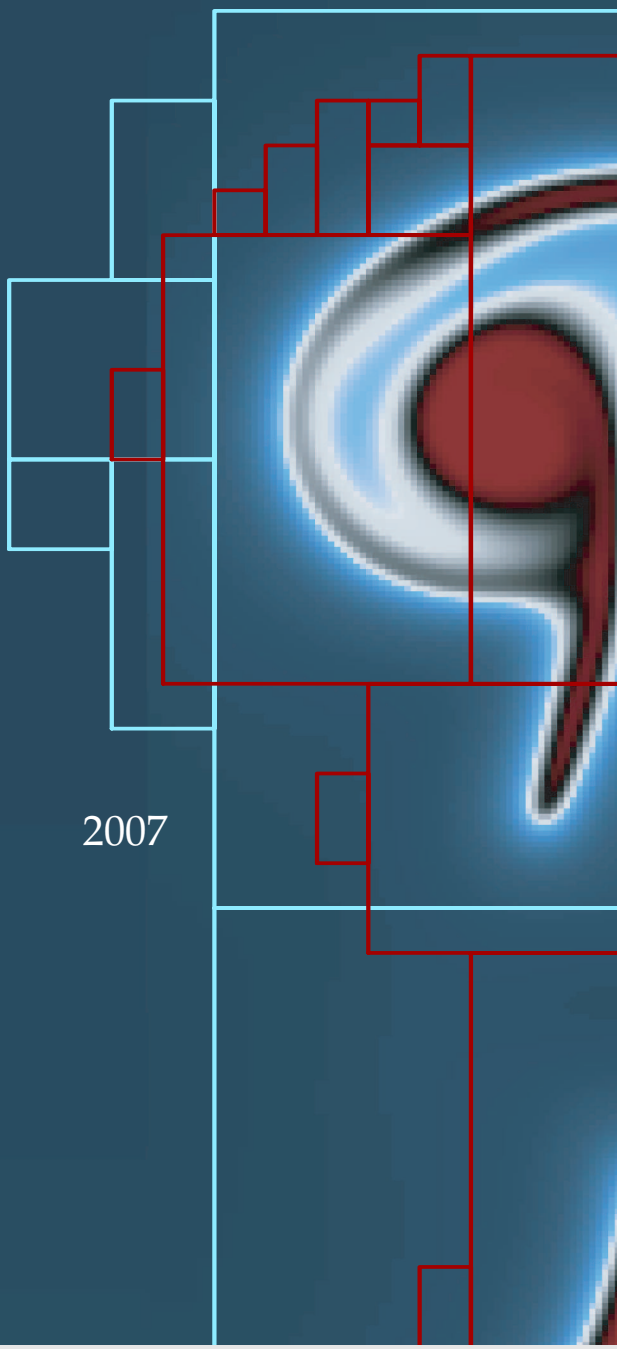

HYBRID NUMERICAL TREATMENT OF TWO-FLUID PROBLEMS WITH PASSIVE INTERFACES

NICHOLAS G. COGAN

mathematical sciences publishers

COMM. APP. MATH. AND COMP. SCI.
Vol. 2, No. 1, 2007

HYBRID NUMERICAL TREATMENT OF TWO-FLUID PROBLEMS WITH PASSIVE INTERFACES

NICHOLAS G. COGAN

We consider the coupled motion of a passive interface separating two immiscible fluids of different viscosities. There are several applications where the velocity of the two fluids is needed everywhere within the domain. Examples include the transport of bacteria and diffusing substances within a biofilm matrix and the transport of cations throughout the mucociliary and periciliary layer in the lung lining. In this investigation, we use a hybrid approach which employs the boundary integral method to determine the interface velocity and the method of regularized stokeslets to determine the velocity elsewhere in the domain.

Our approach capitalizes on the strengths of the two methods, yielding an intuitive, efficient procedure for determining the velocity of a two-fluid system throughout the domain. A key feature of the method is the extension to two-fluid systems with varying viscosity. We describe the results of three numerical simulations designed to test the numerical method and motivate its use.

1. Introduction

We consider the dynamics of two immiscible fluids of different viscosities separated by a passive interface. The motion of both fluids is assumed to be dominated by viscosity and described mathematically by the incompressible Stokes equations. In the absence of a background flow the fluids move because of stress differences at the interface that arise due to different viscosities. Due to the linearity of Stokes equations, the dynamics of the system with a background flow is the superposition of the motion due to jump in the traction across the interface and the background motion of the fluids.

Though the fluid equations are linear, the coupling between two fluids renders the full system nonlinear. Moreover, the interface between the fluids is typically heterogeneous and not aligned with a regular grid, complicating numerical approximations as well as being time-dependent. In particular, standard grid-based methods are

MSC2000: 76B70.
Keywords: two-fluid, boundary integral method, regularized stokeslets, biofilm.
This work is supported in part by NSF grant DMS #0548511.

prone to large approximation errors while standard finite element methods require substantial computation in order to triangulate the dynamic domain.

Several methods have been introduced to address these issues [2; 10; 11; 12; 17]. One class of these methods transforms the equations into integral equations and then attempts to solve the integral equations as accurately as possible, with the least computational effort. In [2; 10], methods are developed to produce solutions that are second order accurate both on and near the interface. The main idea is to take a standard quadrature approximation of the solution to the integral equation and add a correction term. This correction term is computed using asymptotic analysis of the error due to smoothing of the nearly singular kernel and that due to discretization of the integral equation. It is shown that a second order accurate method can be developed in this manner. In [12], the computational effort was addressed. A fast multipole method was introduced to solve the integral equation associated with the bi-harmonic equation. This method requires $\mathcal{O}(N)$ operations, where N is the number of points in the discretization.

Rather than transform the equations into integral equations, a different class of methods attempts to solve the associated primitive variable formulation using finite difference methods. For typical applications there is a jump in the material properties across a curve in the domain. This jump introduces unacceptable errors in the solution via standard finite difference discretization. In [11; 17], the standard finite difference stencil is altered for points near the interface in order to maintain the accuracy. LeVeque and Li [11] introduced a method incorporating the interface jump condition into the discretized Laplacian operator. The resulting scheme is second order accurate. Wei et al. [17] introduced a method termed the matched interface and boundary method. Rather than use the jump condition to alter the discretization, this method uses the jump conditions iteratively. At irregular points on the grid (i.e., those whose finite difference stencil overlaps the two regions), values of the stencil are given at fictitious grid points and are iteratively determined to satisfy the lowest order approximate jump condition. This subtle difference allows for the generation of discretizations of very high order.

The overall method described in this report is a hybrid method that uses different methods to determine the velocities at points on the interface and points within the domain, but away from the interface. We use the well described boundary integral method (BIM) to evaluate the velocity at the interface. These velocities are used as data for the method of Regularized Stokeslets (RS) to obtain the velocity at points on a regular background grid. This hybrid approach is an efficient method that capitalizes on the strengths of each of these methods and is a conceptually straightforward method for tracking the dynamics of a two-fluid system. Although the method is applicable in higher dimensions, for simplicity we will restrict our domain to two dimensions throughout.

We organize the manuscript as follows: the first sections introduce the notation and governing equations and briefly describe the methods that are used. The purpose of this investigation is not to develop more powerful implementations of these methods, but to describe how to use each of them to increase the efficiency of the numerical simulations. Therefore we describe the methods briefly and describe the development of the numerical method; we then focus on several simulations aimed at validating and applying the numerical methods and finally summarize the results. The focus of this report is on the development of the method rather than the applications which will be described elsewhere; hence we give two examples where this method is applicable.

2. Derivation of the hybrid approach

2.1. ***Model equations.*** We consider the coupled motion of two fluids of different viscosities. We assume that viscosity dominates both fluids, so the inertial terms may be neglected. The fluids occupy a region Ω and are separated by a surface, Γ. We denote the two sub-regions as $\Omega^{(1)}$ and $\Omega^{(2)}$ for the external and internal fluids, respectively.

The dynamics of both fluids are governed by the incompressible Stokes equations

$$\nabla \cdot \sigma^{(*)} = \mathbf{F} \tag{1}$$

$$\nabla \cdot \mathbf{U}^{(*)} = 0, \tag{2}$$

where $* = 1, 2$ denotes variables in the external and internal regions, respectively, $\mathbf{U}$ is the velocity vector and $\mathbf{F}$ denotes an applied force . Stokes equations describe conservation of momentum and mass with stress tensors $\sigma^* = -P^*\mathbf{I} + \mu^*(\nabla\mathbf{U}^* + \nabla\mathbf{U}^{*\mathbf{T}})$ that contain both the hydrostatic pressures, P^*, and the viscous stresses proportional to the deformation gradient tensor with viscosities μ^* that are generally different.

The solution to Equations (1) and (2) when $\mathbf{F}$ is a force applied at a single point, $\mathbf{F} = \mathbf{f}\delta(\mathbf{x} - \mathbf{x_0})$, is referred to as a *stokeslet* or the Greens' function. The key property of Stokes equations that is exploited by both BIM and RS is the existence of a functional representation of the stokeslet for a variety of domains [13]. The free space Green's function, $\mathbf{G}$, in two dimensions is,

$$\mathbf{G}_{ij}(\mathbf{x}) = -\delta_{ij} \ln r + \frac{(\mathbf{x} - \mathbf{x_0})_i (\mathbf{x} - \mathbf{x_0})_j}{r^2}. \tag{3}$$

The related stress tensor,$\mathbf{T}$, is,

$$\mathbf{T}_{ijk} = -4\frac{(\mathbf{x} - \mathbf{x_0})_i (\mathbf{x} - \mathbf{x_0})_j (\mathbf{x} - \mathbf{x_0})_k}{r^4}, \tag{4}$$

where $r = |\mathbf{x} - \mathbf{x_0}|$.

Instead of using the free-space Green's function we could use the Green's function that enforces the zero-flow boundary condition by subtracting image singularities if the domain is bounded (e.g. channel flow) [13]. We also note that $\mathbf{G}$ and $\mathbf{T}$ are often referred to as the single and double layer potentials, respectively.

2.2. ***Boundary integral method.*** The boundary integral method (BIM) exploits the linearity of the basic flows and translates the differential equations (1) and (2) to integral equations determining the velocities within the domain. These are used along with continuity of the flow to determine an integral equation that determines the velocity of the interface. This method has several advantages including reduction in the dimensionality of the problem, ability to handle generic interfaces and incorporation of different material properties [15; 6].

To derive the BIM equations, we relate the unknown velocity $\mathbf{U}^*$ to the flow induced by a singular force with intensity $\mathbf{f}$ at a point $\mathbf{x_0}$, $\mathbf{U}'$. Thus $\mathbf{U}'$ is a fundamental solution to the incompressible Stokes equations

$$\nabla \cdot \sigma' = \mathbf{f}\delta(\mathbf{x} - \mathbf{x_0}) \tag{5}$$

$$\nabla \cdot \mathbf{U}' = 0, \tag{6}$$

where $\sigma' = -P\mathbf{I} + \mu(\nabla\mathbf{U} + \nabla\mathbf{U}^{\mathbf{T}})$. This is a convenient flow to use since the solution is given by Equation (3).

The reciprocal relation for the bulk flow is determined by relating solutions to Equations (1) and (2), with $\mathbf{F} = 0$, to (5), (6). By direct calculation, we find that

$$\nabla \cdot (\mathbf{U}\sigma') - \nabla \cdot (\mathbf{U}'\sigma) = \delta(\mathbf{x} - \mathbf{x_0})\mathbf{U}, \tag{7}$$

which is the classical reciprocal relation.

Integrating the reciprocal relation, with various placements of the singular force, we recast Equations (1) and (2), with $* = 1$, as an integral equation whose domain is the interface Γ. The integral equation relates the bulk fluid velocity to the traction jump across the interface, denoted $\Delta\sigma = (\sigma^{(1)} - \sigma^{(2)})$, and the velocity; see [13, Chapter 5]. The motion of the bulk fluid is

$$\mathbf{U}_j^{(1)}(\mathbf{x_0}) = -\frac{1}{4\pi\mu^{(1)}} \int_\Gamma \Delta\sigma_{ik}\eta_k(\mathbf{x})\mathbf{G}_{ij}(\mathbf{x}, \mathbf{x_0})\, dl(\mathbf{x}) + \frac{1-\lambda}{4\pi} \int_\Gamma \mathbf{U}_i(\mathbf{x})\mathbf{T}_{ijk}(\mathbf{x}, \mathbf{x_0})\eta_k(\mathbf{x})\, dl(\mathbf{x}), \tag{8}$$

where $\lambda = \dfrac{\mu^{(2)}}{\mu^{(1)}}$ and we denote the outward normal to the interface as η.

Equation (8) governs the j-th component of the external fluid velocity. In a similar manner, we obtain an integral equation for the motion in $\Omega^{(2)}$,

$$\mathbf{U}_j^{(2)}(\mathbf{x_0}) = -\frac{1}{4\pi\mu^{(1)}\lambda}\int_\Gamma \Delta\sigma_{ik}\eta_k(\mathbf{x})\mathbf{G}_{ij}(\mathbf{x},\mathbf{x_0})\,dl(\mathbf{x}) + \frac{1-\lambda}{4\pi\lambda}\int_\Gamma \mathbf{U}_i(\mathbf{x})\mathbf{T}_{ijk}(\mathbf{x},\mathbf{x_0})\eta_k(\mathbf{x})\,dl(\mathbf{x}). \quad (9)$$

These two integral equations govern the coupled motion of the external and internal materials. Because the flows must be continuous at the boundary, we can obtain the boundary velocity by taking the limit of (8) and (9) as $\mathbf{x}_0$ moves to the boundary. These limits both converge to

$$U_j(\mathbf{x}_0) = -\frac{1}{2\pi\mu^{(1)}(\lambda+1)}\int_\Gamma \Delta\sigma_{ik}\eta_k(\mathbf{x})\mathbf{G}_{ij}(\mathbf{x},\mathbf{x_0})\,dl(\mathbf{x}) + \frac{\kappa}{2\pi}\int_\Gamma^{\mathcal{PV}} \mathbf{U}_i(\mathbf{x})\mathbf{T}_{ijk}(\mathbf{x},\mathbf{x_0})\eta_k(\mathbf{x})\,dl(\mathbf{x}), \quad (10)$$

where $\kappa = \frac{1-\lambda}{1+\lambda}$. The latter integral must be handled with care. There are many methods for evaluating this integral that depend on the dimension of Γ as well as the kernel of the integral. In this situation, the singularity is integrable and straightforward quadrature rules work well [14]. The methods used are described in more detail below.

To close the system we impose a constitutive relation relating the jump in traction, $\Delta\sigma$, to the curvature, ω. We assume that the surface traction is proportional to the curvature, with constant of proportionality γ. This constitutive relation is interpreted as a traction arising from surface tension. We note that this is substantially different than what needs to be done in higher dimensions (see [13, Section 5.5] for a description in three-dimensions).

2.3. ***Regularized stokeslets.*** This method, described in [5], is an efficient method to approximate the solution to Stokes equations in the presence of immersed boundaries or obstacles. Conceptually, RS uses the fact that Stokes equations are linear so the velocity at a given point is linearly related to the force applied at that point. Given a collection of points, $\mathbf{x_i}$, at which singular forces are applied , $\mathbf{F} = \mathbf{f}\delta(\mathbf{x}-\mathbf{x_i})$, the total flow is given as the superposition of each of the stokeslets. However, this representation of the velocity is singular at each of the points. In RS, the forces are applied over a small ball, regularizing Stokes equations. The forces are given by $\mathbf{F} = \mathbf{f}\phi_\epsilon(\mathbf{x}-\mathbf{x_0})$, where ϕ_ϵ is a smooth function with support ϵ. For particular choices of ϕ_ϵ, analytic expressions for the solution to Stokes equations with regularized forces can be recovered. These 'regularized stokeslets' are analytic

and converge to the classical stokeslet as ϵ tends toward zero. The flow due to a collection of forces is a linear combination of the regularized stokeslets.

A specific blob in three dimensions is

$$\phi_\epsilon(\mathbf{x}) = \frac{3\epsilon^3}{2\pi(|\mathbf{x}|^2+\epsilon^2)^{5/2}}.$$

The corresponding Green's function is

$$G_\epsilon(r) = \frac{1}{2\pi}\left(\ln(\sqrt{r^2+\epsilon^2}+\epsilon) - \frac{\epsilon}{\sqrt{r^2+\epsilon^2}}\right),$$

where $r = |\mathbf{x}-\mathbf{x_i}|$. The velocity at $\mathbf{x}$ due to a collection of forces centered at $\mathbf{x_i}$ is

$$\mathbf{U}(\mathbf{x}) = -\mathbf{f_i}\frac{1}{4\pi\mu}\sum_{i=1}^{N}\left(\ln(\sqrt{r_i^2+\epsilon^2}+\epsilon) - \frac{\epsilon(\sqrt{r_i^2+\epsilon^2}+2\epsilon)}{(\sqrt{r^2+\epsilon^2}+\epsilon)\sqrt{r_i^2+\epsilon^2}}\right) + \frac{1}{4\pi\mu}\big(\mathbf{f_i}\cdot(\mathbf{x}-\mathbf{x_i})\big)(\mathbf{x}-\mathbf{x_i})\left(\frac{\sqrt{r_i^2+\epsilon^2}+2\epsilon}{(\sqrt{r_i^2+\epsilon^2}+\epsilon)^2\sqrt{r_i^2+\epsilon^2}}\right). \quad (11)$$

This relationship can also be used to determine forces that yield particular flows. For example, if the velocities at a collection of N points , $\mathbf{x}_i$, are known, one has $\mathcal{U} = \mathcal{M}\mathcal{F}$. The vectors $\mathcal{U}$ and $\mathcal{F}$ are $2N \times 1$ and $\mathcal{M}$ is a $2N \times 2N$ matrix. Inverting this relation gives the forces in terms of the (known) velocities. It should be noted that $\mathcal{M}$ is typically not invertible. This can be avoided by adding a constant to the normal component of the forces, affecting the pressure but not the velocity [5] and using an iterative solver. We can then reconstruct the velocity everywhere within the domain, since it is a superposition of the background flow and the flow due to the calculated forces. This method can be made second-order accurate everywhere using the techniques described in [2].

2.4. ***Hybrid method.*** Although much work has been done for determining the velocity and evolution of the interface, in many applications, the velocity is needed throughout the domain. In applications where the concentration of advected substances (such as oxygen) is needed throughout the domain such as biofilms [4], the velocity at all points of a regular grid is required.

The general method begins by initializing the interface between the two fluids, Γ. We parameterize the coordinates of the interface by s, $\Gamma(x, y, t) = (x(s,t), y(s,t))$. The interface is discretized into control points and Equation (10) is solved at each of the discrete points. We then use RS to determine the velocity at regular grid points. The velocities can then used to determine the transport of a chemical throughout the domain.

Because the surface traction is assumed to be proportional to the curvature, the right-hand-side of Equation (10) is

$$-\frac{1}{2\pi\mu^{(1)}(\lambda+1)}\int_\Gamma \Delta\sigma_{ik}\eta_k(\mathbf{x})\mathbf{G}_{ij}(\mathbf{x},\mathbf{x_0})\,dl(\mathbf{x}) = -\frac{\gamma}{2\pi\mu^{(1)}(\lambda+1)}\int_\Gamma \omega(\mathbf{G}_{1j}\eta_1+\mathbf{G}_{2j}\eta_2)\,dl(\mathbf{x}).$$

The curvature of the boundary is

$$\omega = \frac{x_s y_{ss} - y_s x_{ss}}{(x_s^2+y_s^2)^{(3/2)}}. \tag{12}$$

The outward normal is calculated using the parameterization of the interface.

To solve Equation (10), we are then confronted with a system of coupled integral equations which can be written as

$$\mathbf{W} = \mathbf{b} + \frac{\kappa}{2\pi}\int_\Gamma \mathbf{KW}\,dl(\mathbf{x}). \tag{13}$$

where $\mathbf{W} = (\mathbf{U}_1^{(1)}, \mathbf{U}_2^{(1)})$. The vector $\mathbf{b}$ contains the stokeslet and the tensor $\mathbf{K}$ contains the related stress tensor, both of which are known.

A straightforward method for solving the discretized integral equations is Nyström's method [16], which requires a quadrature rule:

$$\int_a^b y(s)ds = \sum_{j=1}^{n}\omega_j y(s_j),$$

where ω_j denotes the weights of the quadrature rule. For our simulations we use Gauss-Legendre quadrature. Although the kernel of Equation (13) has an integrable singularity, it has been shown that the convergence of Nyström's method is the same as the rate of convergence of the quadrature and, if the singularity is of a known type, the rate of convergence can be increased by correcting the quadrature weights [1]. We note that we do not use this acceleration technique in the present investigation.

Once we have solved this system, we have the velocity of the interface at the discrete control points. We could proceed in a similar manner and find the velocity at each point in a regular lattice using Equations (8) and (9). Instead we use the method described above. We first determine the forces that must be applied to the fluid in $\Omega^{(1)}$ so that the velocities at the control points on the interface match those obtained by the BIM. Using these forces and Equation (11), we find the velocities at regular grid points in $\Omega^{(1)}$. The forces required to force the internal fluid to match the velocity of the interface are proportional to the forces obtained for the external fluid and we can then determine the velocity within $\Omega^{(2)}$. The velocities are continuous at the interface and both agree with the velocity found using BIM.

This hybrid method is computationally less expensive than naive implementation of the boundary integral method. The operation count using the BIM equation to determine the velocity at each point on a regular $(M \times M)$ grid using a trapezoidal approximation of the integral, with N discrete points on the interface, is $\mathcal{O}(N^3M^2)$ for each time step. For the RS the operation count is $\mathcal{O}(N^2 + NM^2)$ since each time step requires a matrix inversion (using GMRES $\mathcal{O}(N^2)$ and the summation of the stokeslet solutions for each of the N control points at each of the M^2 points on the regular grid). Thus in problems which require the velocity at all points on a background grid, the interface can be accurately discretized without undo cost.

It should be noted that the above discussion does not consider less naive methods for solving the integral equations that arise from BIM. There are several techniques that are used to reduce the operation count. In particular fast summation multipole methods can be much less computationally expensive [2; 12]. Using these methods the operation count for using BIM alone can be reduced to $\mathcal{O}(NM^2)$ for each time step. Thus for problems for which the fluid flow throughout the domain is needed accurately throughout the domain (i.e., where M is much large than N), BIM with multipole methods can be slightly better than the hybrid method. In our simulations it is typical to have $N = 100$, while $M = 250$ so that the relative difference in the orders is very small, about 0.5%.

3. Simulations

3.1. ***Steady flow.*** We first describe the numerical results of applying the method for a single time step to validate the implementation of Nyström's method as well as demonstrate the behavior of the method for systems with differing viscosities. We begin with a square domain located at $(-2, 2) \times (-2, 2)$. A fluid of viscosity μ_{int} located at the interior of a circle of radius one. The fluid outside of the circle has viscosity μ_{ext}. We use methods described in [10] to derive an analytic solution to the problem with given forces. We parameterize the circle by $\mathbf{x} = (\cos(\theta), \sin(\theta))$ and take the analytic solutions given in [5] and scale the pressure with the internal and external viscosities.

The analytic representation of the pressure and velocities, namely

$$p(r,\theta) = \begin{cases} \mu_{\text{ext}} r^{-3} \sin(3\theta) & \text{for } r \geq 1, \\ \mu_{\text{int}} r^{3} \sin(3\theta) & \text{for } r < 1, \end{cases}$$

$$u_1(r,\theta) = \begin{cases} \frac{1}{8} r^{-2} \sin(2\theta) - \frac{3}{16} r^{-4} \sin(4\theta) + \frac{1}{4} r^{-2} \sin(4\theta) & \text{for } r \geq 1, \\ \frac{3}{8} r^{2} \sin(2\theta) + \frac{1}{16} r^{4} \sin(4\theta) - \frac{1}{4} r^{2} \sin(2\theta) & \text{for } r < 1, \end{cases}$$

$$u_2(r,\theta) = \begin{cases} \frac{1}{8} r^{-2} \cos(2\theta) + \frac{3}{16} r^{-4} \cos(4\theta) - \frac{1}{4} r^{-2} \cos(4\theta) & \text{for } r \geq 1, \\ \frac{3}{8} r^{2} \cos(2\theta) - \frac{1}{16} r^{4} \cos(4\theta) - \frac{1}{4} r^{2} \cos(2\theta) & \text{for } r < 1, \end{cases}$$

are used in the equations

$$[\sigma_{ij}]\eta_j = -f_i, \text{ for } i = 1, 2,$$

to calculate the boundary forces. Here the stress tensor σ is

$$\sigma_{ij} = -p\delta_{ij} + \mu\left(\frac{\partial u_i}{\partial x_j} + \frac{\partial u_j}{\partial x_i}\right).$$

For our calculations we prescribe the boundary forces at discrete points representing the boundary and solve Equation (13) to determine the boundary velocities. The velocities at the control points are used to determine the forces to apply to the fluid regions to match the calculated velocities which in turn is used to determine the external and internal velocities via the RS. Because we are only considering the steady problem for prescribed boundary forces we do not need to use the curvature constitutive assumption to specify the boundary traction. Instead, $\nabla\sigma_{ij}\eta_j = f_i$

To consider the convergence of the numerical approximation to the exact solution, we allow the the number of points discretizing the interface, N, to increase while the background grid used to determine the velocity away from the interface is fixed. Following [5], we measure the error along the line $(x, 3/10)$. We first consider the case where the viscosities are equal as in [5] (see Table 1). The velocity field and the x- and y- components of the velocity along the line $(x, 3/10)$ are shown in in Figure 1. By comparing the ratios of the errors as the number of interface points is doubled we find the order of the comparison. For a first order method the ratio is two while a second order method would have a ratio of four. These ratios are provided in the tables indicating that the method is between first and second order for each of the examples.

Next, we consider the behavior when the viscosities of the two fluids are not equal. In general the convergence rate is reduced as the jump in the viscosity increases . The results for two simulations with different viscosities are summarized in Tables 2 and 3. To determine the rate of convergence we compare the errors for subsequent refinements. We note that this convergence would be improved if the methods in [2] were implemented; however, our results are in agreement with those in [5] for the single viscosity case.

# boundary points	L_2 error in u_1	ratio	L_2 error in u_2	ratio
$N = 50$	2.99×10^{-2}		3.14×10^{-2}	
$N = 100$	7.89×10^{-3}	3.7896	6.46×10^{-3}	4.8606
$N = 200$	1.83×10^{-3}	4.3833	1.03×10^{-3}	6.2718
$N = 400$	4.47×10^{-4}	4.0268	3.53×10^{-3}	2.9178

Table 1. Velocity errors: $\mu_1 = \mu_2 = 1$.

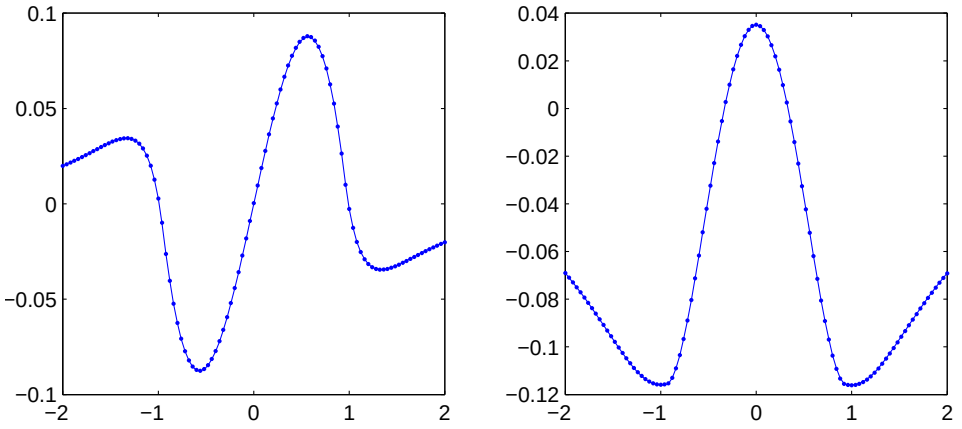

Figure 1. Comparison of the analytic velocities (solid) and the numerical approximation (dotted) along the line $(x, 3/10)$. Left caption shows u_1 while the right shows u_2. The background mesh has 100×100 points and the boundary is discretized with 200 points. The solution is being approximated well.

3.2. ***Viscous suctioning.*** We have just computed the approximate solution for a single time step. To determine the behavior of the numerical methods for a moving boundary, we choose to examine a problem that is similar to the well known Hele-Shaw problem with a singular sink term [3]. Here, we consider the flow of a two-fluid system where an initially circular blob of fluid with viscosity μ_2 is

# boundary points	L_2 error in u_1	ratio	L_2 error in u_2	ratio
$N = 50$	3.33×10^{-2}		2.42×10^{-2}	
$N = 100$	8.86×10^{-3}	3.7584	9.76×10^{-3}	2.4795
$N = 200$	2.54×10^{-3}	3.4881	2.50×10^{-3}	3.9040
$N = 400$	9.67×10^{-4}	2.6266	6.17×10^{-4}	4.0518

Table 2. Velocity errors: $\mu_1 = 1$, $\mu_2 = 2$.

# boundary points	L_2 error in u_1	ratio	L_2 error in u_2	ratio
$N = 50$	2.68×10^{-2}		5.06×10^{-2}	
$N = 100$	9.94×10^{-3}	2.6962	1.96×10^{-2}	2.5816
$N = 200$	4.78×10^{-3}	2.0795	8.90×10^{-3}	2.2022
$N = 400$	1.50×10^{-3}	3.1867	4.35×10^{-3}	2.0460

Table 3. Velocity errors: $\mu_1 = 1$, $\mu_2 = 5$.

immersed in a viscous fluid of viscosity μ_1. The circle is initially of radius one and centered at the origin. At time $t = 0$, we initiate a singular sink term at a point interior to the circle that draws the interior fluid out of the domain causing motion of the interface and the external fluid. This problem has been treated in many investigations (see [7] for analytic treatment and references). In general, in the absence of surface tension there is a singularity in finite time whenever $\mu_2 > \mu_1$. With small surface tension, the problem is regularized and various smooth solutions can be found depending on the location of the sink relative to the circle as well as the strength of the point-sink.

To include a singular sink term in our scheme, we consider the background flow that is the solution to

$$\Delta \mathbf{U} = \nabla p,$$
$$\nabla \cdot \mathbf{U} = q\delta(\mathbf{x} - \mathbf{x_0}),$$

namely

$$\mathbf{U}_{\text{suction}} = q \frac{\mathbf{x} - \mathbf{x_0}}{|\mathbf{x} - \mathbf{x_0}|}.$$

This is added to the flow obtained due to the interface motion to give the motion of the interface.

The computational domain $[-1.5, 1.5] \times [-1.5, 1.5]$ is discretized into a regular background grid with 200×200 grid points. This initial interface is a circle of radius one centered at the origin. There are 150 regularly spaced control points. The viscosities are $\mu_1 = 1$ and $\mu_2 = .1$, for the internal and external viscosities, respectively. The analytic studies rely on complex function theory and mapping techniques to determine the dynamics of the interface. In general, our method is able to capture, qualitatively, the behaviors that are found analytically. We are also able to determine the velocities throughout the domain. In particular, the solutions exhibit singularities at a time, $t_b(\gamma)$, that depends on the value of the surface tension. In our simulations, t_b is an increasing function of γ, indicating the role of surface tension regularization. We have not done a complete investigation of the behavior as a function of surface tension as that is not the focus of this investigation; however, we show the velocity of the fluids near the developing cusp to indicate that our method can capture the fluid flow near the interface as well as the motion of the interface. The results for various simulations are shown in Figures 2 and 3.

3.3. ***Advection.*** One strength of the method described above is efficient approximation of the velocity everywhere in the domain. This is important in transport problems such as biofilm disinfection, where the main goal is to determine the concentration of biocide and nutrient as it moves in the bulk fluid and into the

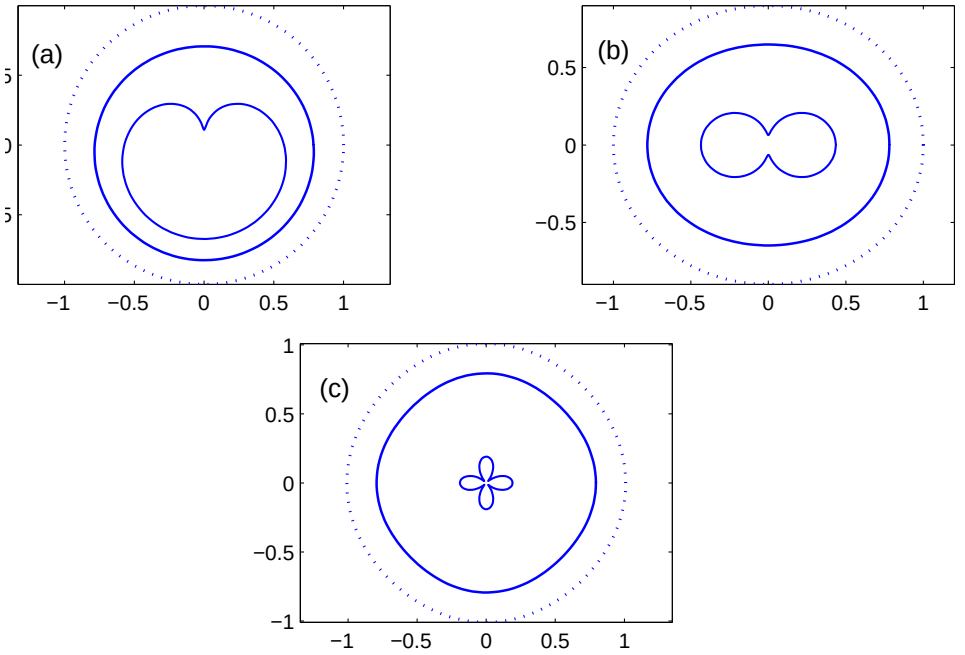

Figure 2. Results for viscous suctioning. (a) Initially circular interface with singularity at $(0, 0.1)$. (b) To break the symmetry, we perturb the circle into an ellipse with major axis 1 and minor axis 0.9 in the y-direction. The singularity is placed at the origin. (c) To break the symmetry, we perturb the circle by adding a periodic fluctuation in the radius with amplitude .01. The singularity is placed at the origin. In all simulations the $\mu_1 = 1$ and $\mu_2 = 0.1$ and the initial interface is indicated with the dotted line while the other curves are shown after 100 and 250 time steps.

biofilm domain. Several models treat the biofilm as a viscous fluid with a viscosity that is substantially different than that of the external fluid [4; 9; 8].

The domain is a channel with a parabolic background flow. Within the channel a generic biofilm interface separates the biofilm fluid, with viscosity $\mu_{biofilm}$ from the bulk fluid with viscosity μ_{bulk}. Although biofilms display viscoelastic properties, the relaxation time has been measured to be on the order of minutes [9]. Because transport of biocide within the biofilm typically takes place on a time scale of hours to days, we treat the biofilm as a viscous fluid immersed in a fluid of much less viscosity [8]. Measurements of biofilm viscosity indicate that the viscosities differ by several orders of magnitude [9]. We set $\mu_{biofilm} = \mu_{bulk} \times 10^6$ and impose a parabolic background flow which is altered by the presence of the biofilm.

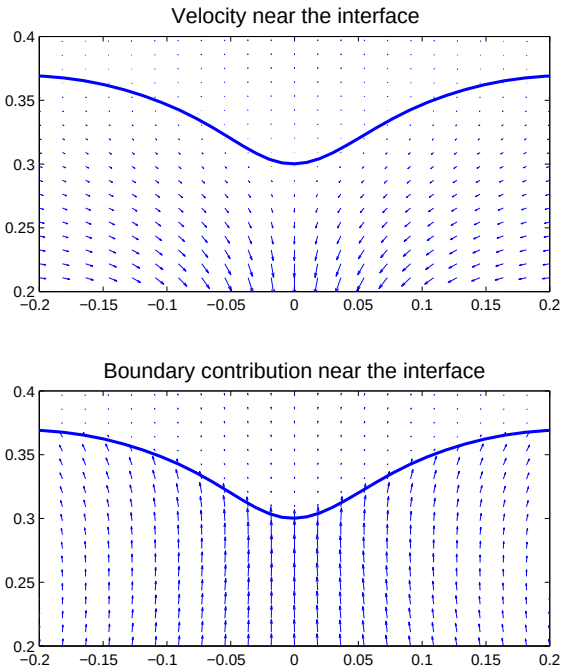

Figure 3. Zoom in of the internal and external velocity field near the forming cusp in Figure 2(a). The top figure shows the total velocity, while the bottom shows the contribution from the interface (without the background flow). Note that the scales have been altered for visualization and do not reflect the magnitudes.

Following the methods described above, we determine the velocity of the interface and fluid in both the bulk and biofilm regions. This is used to track the advection and diffusion of a chemical whose concentration, C, is determined mathematically by a conservation law

$$\frac{\partial C}{\partial t} + (\mathbf{U} \cdot \nabla)C = D\Delta C,$$

where the concentration is fixed at C_0 at the leading edge of the channel. No-flux and outflow conditions are applied at the channel walls and trailing edge of the channel. Given the velocity at time t we determine the concentration at time $t + \Delta t$ using upwinding and ADI to solve the discretized equation.

In Figure 4 we show the developing concentration contours as well as the biofilm/bulk fluid interface for various times. We plan to indicate the effects of including the motion of the biofilm in a future investigation.

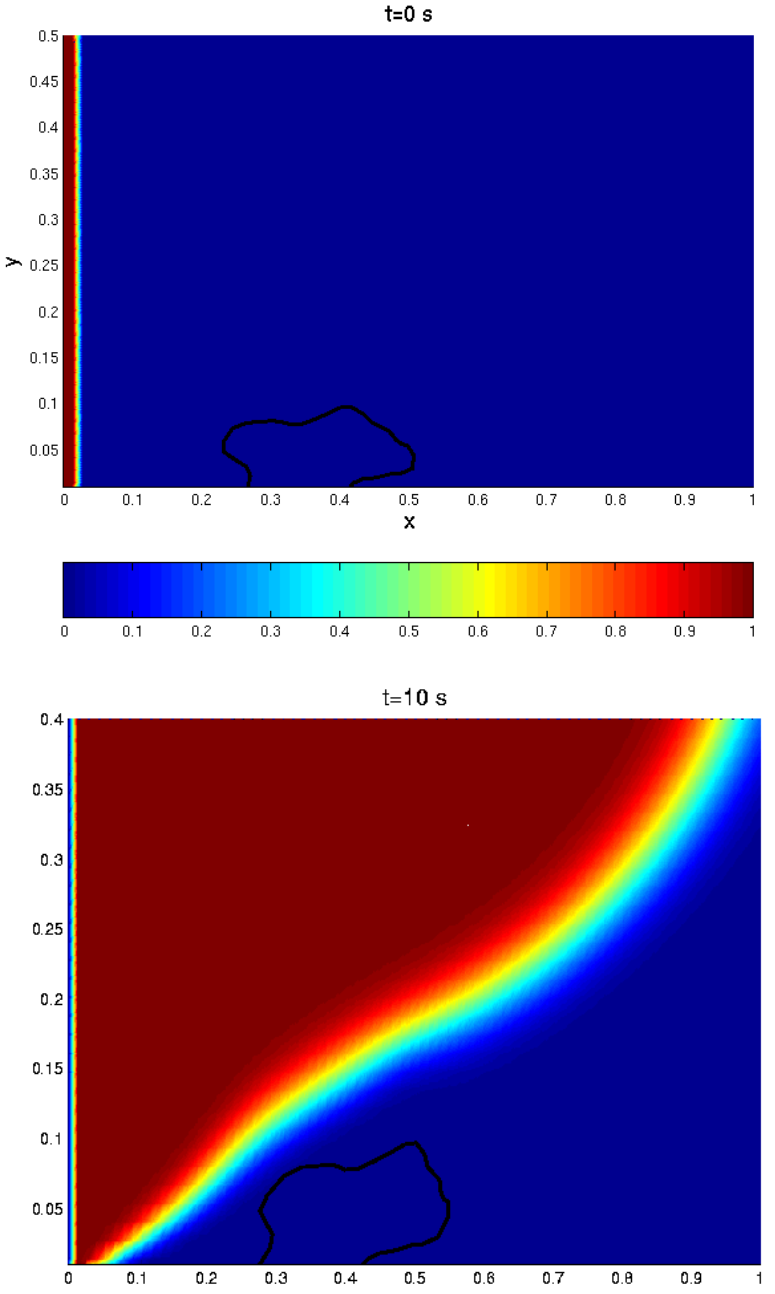

Figure 4. Time-dependent concentration profiles indicating the diffusion and advection of a chemical through the two-fluid domain. We show only part of the domain: $[0, 1] \times [0, 0.4]$. The dynamic fluid/biofilm interface is in black and the concentration for all figures is indicated by the colorbar.

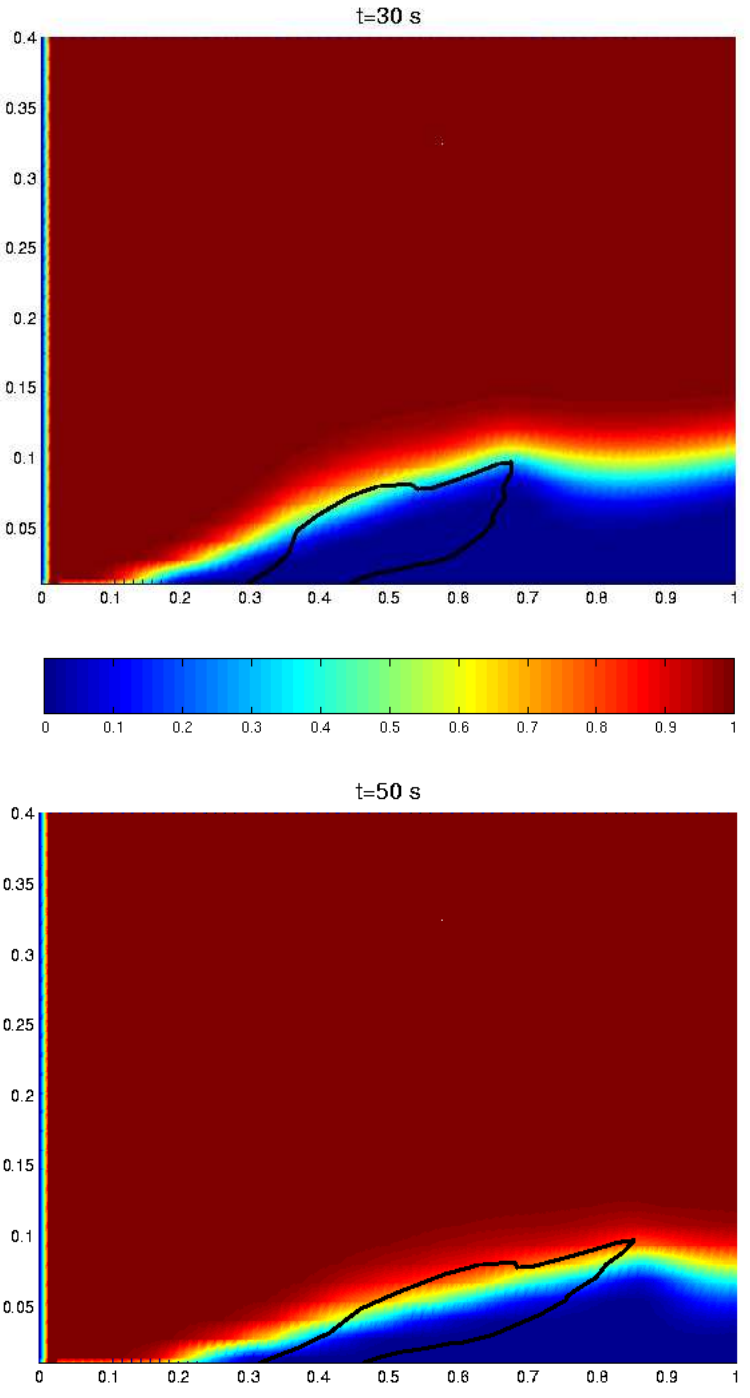
t=30 s
0.4
0.35
0.3
0.25
0.2
0.15
0.1
0.05
0 0.1 0.2 0.3 0.4 0.5 0.6 0.7 0.8 0.9 1
0 0.1 0.2 0.3 0.4 0.5 0.6 0.7 0.8 0.9 1
t=50 s
0.4
0.35
0.3
0.25
0.2
0.15
0.1
0.05
0 0.1 0.2 0.3 0.4 0.5 0.6 0.7 0.8 0.9 1

4. Discussion

This investigation describes the development of a hybrid method for numerically approximating the motion to two viscous fluids separated by an interface. The interface velocity at control points is determined by solving an integral equation. The velocity at the control points is then used as data to determine the flow outside and inside the interface using the RS. Our method capitalizes on the strengths of both of the methods, since RS is an efficient method but leads to errors at the interface which is precisely where BIM is being applied. We have also indicated that the computational complexity of the hybrid approach is comparable to fast multipole methods applied to BIM, motivating the use of the method for problems where the total flow is needed. We also feel that this investigation indicates an area where the strengths of various methods including RS, multipole methods and matched boundary methods can be exploited.

To apply the numerical method, we studied three different problems. The first was a static problem for which there is an analytic solution. We found that when the viscosities of the fluids are equal, the method behaves as in [5]. However, we have extended the treatment to case with differing viscosities. We then treated a viscous suctioning problem where we were able to capture the qualitative nature of the development of cusps. More importantly for this method, we were able to examine the velocity near the interface. Both the total flow and the flow without the background flow are readily calculated. Finally, we applied our method to determine the concentration of a chemical as it diffuses and advects throughout a channel filled with two immiscible fluids of extremely different viscosities. The last example is the motivation for the numerical method. In particular, the efficiency of the method is desirable since in this situation, the simulations must be carried out for relatively long times (hours, whereas a typical time scale is on the order of seconds to minutes). Other applications where this method could be of use include the diffusion of various cations through the mucociliary layer and into the periciliary layer lining the lungs. This transport problem is a necessary component toward understanding the production and motion of the mucous lining, in particular, for Cystic Fibrosis patients. Reports of the application of this method for more practical problems will be described elsewhere.

References

[1] Bradley K. Alpert, *High-order quadratures for integral operators with singular kernels*, Journal of Computational and Applied Mathematics **60** (1995), 367–378.

[2] J. T. Beale and M.-C. Lai, *A method for computing nearly singular integrals*, SIAM J. Numer. Anal. **38** (2001), 1902–1925.

[3] Hector D. Ceniceros, Thomas Y. Hou, and Helen Si, *Numerical study of Hele-Shaw flow with suction*, Physics of Fluids **11** (1999), no. 9, 2471–2486.

[4] N. G. Cogan and James P. Keener, *The role of the biofilm matrix in structural development*, Mathematical Medicine and Biology **21** (2004), no. 2, 147–166.

[5] Ricardo Cortez, *The method of regularized stokeslets*, SIAM J. Sci. Comput. **23** (2001), no. 4, 1204–1225.

[6] Vittorio Cristini, Jerzy Blawzdziewicz, and Michael Loewenberg, *Drop breakup in three-dimensional viscous flows*, Phys. Fluids Letters **10** (1998), 1781–1783.

[7] L. J. Cummings and S. D. Howison, *Two-dimensional Stokes flow with suction and small surface tension*, European Journal of Applied Mathematics **10** (1999), 681–705.

[8] Isaac Klapper, *Effect of heterogeneous structure in mechanically unstressed biofilms on overall growth*, Bulleting of Mathematical Biology **66** (2004), 809–824.

[9] Isaac Klapper, C.J. Rupp, R. Cargo, B. Purvedorj, and P. Stoodley, *Viscoelastic fluid description of bacterial biofilm material properties*, Biotechnology and Bioengineering **80** (2002), no. 3, 289–296.

[10] Anita T. Layton, *An explicit jump method for the two-fluid stokes equations with an immersed elastic boundary*, Elsevier Science (2006), Submitted.

[11] R. J. Leveque and Z. Li, *Immersed interface methods for Stokes flow with elastic boundaries or surface tension*, SIAM J. Sci. Comput. **18** (1997), 709–735.

[12] A. Mayo, *Fast high order accurate solution of Laplace's equation on irregular regions*, SIAM J. Sci. Comput. **6** (1985), 144–157.

[13] C. Pozrikidis, *Boundary integral and singularity methods for linearized viscous flow*, Cambridge University Press, 1992.

[14] ———, *Interfacial dynamics for stokes flow*, Journal of Computational Physics **169** (2001), 250–301.

[15] ———, *Modeling and simulation of capsules and biological cells*, Chapman & Hall/CRC Press, 2003.

[16] William T. Vetterling, Saul A. Teukolsky, WIlliam H. Press, and Brian Flannerly, *Numerical recipes in c: The art of scientific computing*, Cambridge University Press, Caqmbridge, 2002.

[17] Y.C. Zhoua, Shan Zhaoa, Michael Feig, and G.W. Wei, *High order matched interface and boundary method for elliptic equations with discontinuous coefficients and singular sources*, Journal of Computational Physics **213** (2006), no. 1, 1–30.

Received November 13, 2006.

NICHOLAS G. COGAN: cogan@math.fsu.edu
Department Mathematics, Florida State University, 208 Love Building, Tallahasse, FL 32306-4510
www.math.fsu.edu/∼cogan